Analysis of Dither in Relay Feedback Systems

Luigi Iannelli, Karl Henrik Johansson,
Ulf Jönsson, Francesco Vasca

2002-02-06

IR–S3–REG–0201

ROYAL INSTITUTE
OF TECHNOLOGY
Department of
Signals, Sensors & Systems
Automatic Control
SE-100 44 STOCKHOLM

KUNGL TEKNISKA HÖGSKOLAN
Institutionen för
Signaler, Sensorer & System
Reglerteknik
100 44 STOCKHOLM

Abstract

Dither signals provide an effective way of compensating for nonlinearities in control systems. The seminal works by Zames and Shneydor and more recently by Mossaheb present rigorous tools for systematic design of dithered systems. Their results rely however on a Lipschitz assumption on the nonlinearity and thus do not cover important applications with discontinuities. This paper presents initial results on how to analyze and design dither in nonsmooth systems. In particular, it is shown that a dithered relay feedback system can be approximated by a smoothed system. Guidelines are given for tuning the amplitude and the period time of the dither signal, in order to stabilize the nonsmooth system.

1 Introduction

The use of dither signals for stabilization of nonlinear control systems is a well-known and frequently used technique. The idea is that by injecting a suitably chosen high-frequency signal in the control loop, the nonlinear sector is effectively narrowed and the system can thereby be stabilized. Theoretical justification of this idea for systems with continuous nonlinearities has been obtained by Zames and Shneydor [1, 2] and Mossaheb [3]. Their results rely however on a crucial Lipschitz assumption on the nonlinearity and thus do not cover important applications with discontinuities. Indeed, discontinuous nonlinearities in feedback control systems with high-frequency excitations appear in a large variety of models, including systems with adaptive control [4], friction [5, 6], pulse-width modulated converters [7], quantizers [8], relays [9], and variable-structure controllers [10]. In their paper on the analysis of the (smooth) LuGre friction model, Pervozvanski and Canudas de Wit [11] point out that a rigorous analysis of dither in discontinuous systems does not exist. Dither tuning in nonsmooth systems is to our knowledge limited to approximate design methods mainly based on describing functions [12].

The contribution of the paper is an initial attempt to develop a theory for the design of dither in nonsmooth systems. We limit the analysis to an important class of nonlinearities and dither signals, namely, relay systems with triangular dither signals. The reason for this is that these systems are common, see references above. Our main result states that a dithered relay feedback system can be approximated by a system with no dither and the relay replaced by a saturation. The dither period determines the accuracy of the approximation. The dither amplitude

determines the gain of the saturation and thus the stability of the smoothed system. Exponential stability of the smoothed system is linked to practical stability of the dithered system through a theorem based on a frequency response criterion similar to the circle and Popov criteria. The theoretical results suggest a procedure for tuning dither systems.

The outline of the paper is as follows. Some notation is introduced in Section 2. A motivating example is presented in Section 3, illustrating how a high-frequency dither signal can be injected to dissolve oscillations in relay feedback systems. The main theorem is presented in Section 4 and it states that the solutions of the dithered system can be arbitrarily well approximated by the solutions of a smoothed system. The section also discusses practical stability. Section 5 relates these results to dither design, which is applied to the example. The paper is concluded in Section 6, where topics for future work is discussed.

2 Preliminaries

The dithered system is a relay feedback system

$$\dot{x}(t) = Lx(t) + bn(cx(t) + \delta(t)), \qquad x(0) = x_0. \tag{1}$$

Here L, b, and c are constant matrices of dimensions $q \times q$, $q \times 1$, and $1 \times q$, respectively. The nonlinearity $n : \mathbb{R} \to \mathbb{R}$ is given by the relay characteristic

$$n(z) = \operatorname{sgn}(z) = \begin{cases} 1, & z > 0 \\ 0, & z = 0 \\ -1, & z < 0. \end{cases}$$

The dither signal $\delta : [0, \infty) \to \mathbb{R}$ is a triangle wave of amplitude $A > 0$ and period $p > 0$, i.e., $\delta(t + p) = \delta(t)$ for all t and

$$\delta(t) = \begin{cases} \dfrac{4A}{p}t, & t \in [0, p/4) \\ -\dfrac{4A}{p}t + 2A, & t \in [p/4, 3p/4) \\ \dfrac{4A}{p}t - 4A, & t \in [3p/4, p). \end{cases}$$

Throughout the paper we assume that the relay feedback system has a solution $x : [0, \infty) \to \mathbb{R}^n$ (in a classical sense), which on every compact subinterval of $[0, \infty)$

is C^1 everywhere except at finitely many points. We sometimes use the notation $x(t, x_0)$ for the solution of (1).

The smoothed system is given by

$$\dot{w}(t) = Lw(t) + bN(cw(t)), \qquad w(0) = w_0, \tag{2}$$

where the smoothed nonlinearity $N : \mathbb{R} \to \mathbb{R}$ is defined as the average $N(z) = p^{-1} \int_0^p n(z + \delta(t))dt$. For the relay, it is easy to show that

$$N(z) = \text{sat}(z/A) = \begin{cases} 1, & z > A \\ z/A, & |z| < A \\ -1, & z < -A. \end{cases}$$

It will be shown below that the smoothed system in many cases is a good approximation of the dithered relay feedback system. Therefore analysis and design can be performed on the smoothed system, which is often easier to treat, and then be carried over to the dithered system.

Note that the term "smoothed system" is standard in the literature on dither design and refer to that the nonlinear sector is narrowed by the dither signal. The nonlinearity is not necessarily C^∞, as illustrated above by the saturation function being the smoothed nonlinearity corresponding to the sign function.

We use $|\cdot|$ to denote the Euclidean norm of a vector and $\|\cdot\|$ to denote the corresponding induced matrix norm.

3 A Motivating Example

A second-order relay feedback system is used as a representative example. Consider the system (1) with

$$L = \begin{bmatrix} -2 & -1 \\ 1 & 0 \end{bmatrix}, \quad b = \begin{bmatrix} 1 \\ 0 \end{bmatrix}, \quad c = \begin{bmatrix} 1 & -1 \end{bmatrix}. \tag{3}$$

The linear part of the relay feedback system thus has a nonminimum-phase zero at 1 and a double pole at -1. When no dither is present ($\delta(t) \equiv 0$), the relay feedback system presents a limit cycle as reported in Figure 1. The output of the linear part $-cx$ of (1) is plotted for a solution with initial condition $x_0 = \begin{bmatrix} 2 & 1 \end{bmatrix}^T$.

If we apply a triangle dither signal δ with amplitude $A = 1$ and period $p = 1/50$, the limit cycle in Figure 1 is dissolved as shown in Figure 2. Hence, the

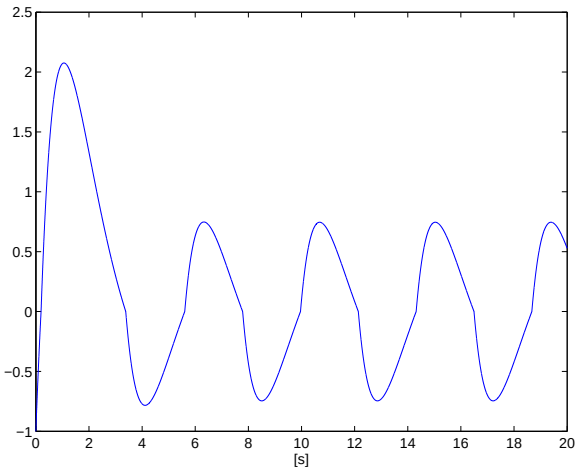

Figure 1: Output $-cx$ of the relay feedback system (1) with (3) but without dither signal ($\delta \equiv 0$).

dither in a sense attenuates the oscillations present in the original system. Figure 2 shows also the output $-cw$ of the smoothed system (2). The two systems have almost identical responses. Hence the smoothed system provides an accurate approximation of the dithered system for $p = 1/50$. Figure 3 shows the responses when the dither signal has a larger period: $p = 1$. The responses are no longer close and the output of the dithered system (solid) is oscillating.

The simulations suggest that the dither period p is related to how accurately the smoothed system approximates the dithered system. In next section it is shown that by choosing p sufficiently small the approximation can be made arbitrarily tight (Theorem 4.1). Regarding the dither amplitude A, note that the smoothed system is unstable for $A < 1/2$, since the closed-loop system is linear with characteristic polynomial equal to $s^2 + (2 - A^{-1})s + 1 + A^{-1}$ when $|cw| < A$. The dither amplitude hence defines the response dynamics. This is shown in next section by relating A to the stability of the dithered system (Theorem 4.2).

4 Main Results

This section presents two result for the dithered system: one on accurate approximation and one on practical stability.

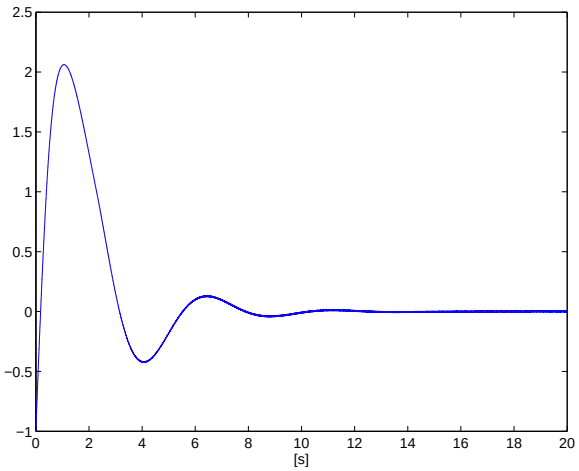

Figure 2: Outputs of the dithered relay feedback system (1) (solid) and the smoothed system (2) (dashed). The responses are almost identical.

4.1 Accurate Approximation

The following theorem states that by choosing the dither period p sufficiently small, it is possible to make the solution x of the relay feedback system arbitrarily close to the solution w of the smoothed system on any compact time interval.

Theorem 4.1. *Let $T, \varepsilon > 0$ and $x_0 \in \mathbb{R}^n$ be given. There exists $p_0 > 0$ such that if $p \in (0, p_0)$, then $|x(t, x_0) - w(t, x_0)| \leq \varepsilon$ for all $t \in [0, T]$.*

Proof. See Appendix A. □

The proof of Theorem 4.1 is constructive, so a bound for p_0 is derived. It shows that p_0 should be chosen to be of the order of ε. The bound depends however also on system data and T. It is conservative, since the derivation is done using no particular knowledge of the system data. Tighter bounds can be obtained by exploiting more of the problem structure, but is not needed for the proof of the theorem.

Theorem 4.1 can be interpreted as an extension of Theorem 1 in [3] to a class of nonsmooth systems. The result in [3] relies on continuity properties of the solutions of the original and the smoothed systems. This argument cannot be used here, since a relay feedback system in general do not have solutions that depend continuously on initial conditions or system parameters. Instead, we pay particular attention in the proof to the system evolution at and between relay switchings.

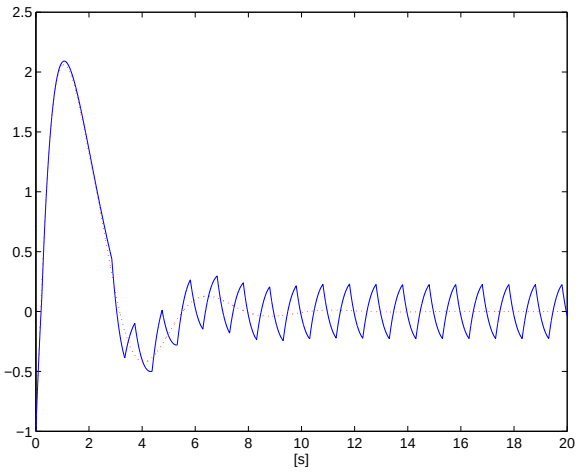

Figure 3: Outputs of the dithered relay feedback system (1) (solid) and the smoothed system (2) (dashed). Similar simulation as in Figure 2 but with dither signal having 50 times longer period. Note the deviation between the responses.

4.2 Practical Stability

We will use Theorem 4.1 to obtain conditions for practical stability of the dithered system (1). The idea is the following. First we choose the amplitude A of the dither signal, such that the smoothed system in (2) is stable. Then if the period p of the dither signal is chosen small enough, the output of the dithered system closely follows the output of the smoothed system. This implies that the output of the dithered system converges close to zero. Note that we cannot obtain convergence strictly to zero, since the dither signal always cause small fluctuations of the output. We use the following definition of stability.

Definition 4.1 (Practical stability). *The system in (1) is called practically (exponentially) stable if for any* $\varepsilon > 0$ *there exists* $A > 0, p_0 > 0, \alpha > 0$, *and* $\beta \geq 1$, *such that*

$$|x(t)| \leq \beta e^{-\alpha t}|x_0| + \varepsilon, \quad \forall t \in [0, \infty)$$

for any dither period $p \in (0, p_0)$.

There are many available results for stability analysis of the smoothed system. We will here use a criterion by Zames and Falb [13], which generalizes the Popov criterion.

Theorem 4.2. *Let $G(j\omega) = -c(j\omega I - L)^{-1}b$ and consider some transfer function $H(j\omega) = \int_{-\infty}^{\infty} h(t)e^{-j\omega t}dt$, where $h : \mathbb{R} \to \mathbb{R}$ satisfies $\int_{-\infty}^{\infty} |h(t)|dt \leq 1$. If there exists $\varepsilon > 0$ such that*

$$\mathrm{Re}\,(G(j\omega) + A)(1 + H(j\omega)) \geq \varepsilon I, \ \forall \omega \in \mathbb{R}, \tag{4}$$

then there exists p_0 such that for $p \in (0, p_0)$ the system (1) *is practically stable.*

Proof. See Appendix B. □

Note that the criterion (4) corresponds to one of the least conservative conditions for stability available for systems with a slope restricted nonlinearity. However, it does not give any immediate information on the performance (e.g., the exponential decay parameters), and it is not convex in the pair A, H. The most straightforward use of the theorem is to put $H = 0$, which corresponds to the circle criterion. From the Kalman–Yakubovich–Popov Lemma one can then derive a linear matrix inequality that verifies (4) and results in explicit estimates of the exponential decay parameters, α_0, β_0, for the smoothed system.

5 Dither Design

In this section we use Theorems 4.1 and 4.2 to design the dither signal, for example, in order to stabilize an oscillation. We also present a heuristic method, which gives less conservative designs. The design methods are illustrated on the example in Section 3.

5.1 Tuning Algorithm

The dither design choice will necessarily be a compromise between conflicting consequences of the dither amplitude A and dither period p on the control performance. Based on our theoretical results we obtain the following algorithm for tuning the parameters of the dither signal.

Step 1 Choose A based on (4) in Theorem 4.2, so that the smoothed system in (2) is exponentially stable.

Step 2 Estimate α_0, β_0 and let $T = -\ln(0.1/\beta_0)/\alpha_0$, where α_0, β_0 are the exponential stability parameters for the smoothed system. Choose p_0 based on T and the smoothed dynamics.

A few comments are in place. In Step 1 we need to choose the amplitude A of the dither signal large enough to allow the smoothed system to be stable and to have fast enough exponential decay rate. At the same time we want to keep A as small as possible in order to avoid injecting a large signal in the control loop.

In Step 2 the estimates of α_0 and β_0 can be derived based on the Kalman–Yakubovich–Popov Lemma, as discussed in Section 4. Then we can compute time interval length T, which is an auxiliary variable in the proof of Theorem 4.2. The parameter T gives a bound on the period of the dither signal through Equation (31) in the proof of Theorem 4.1. The bound is in general quite conservative, since it is derived without using any structure of the problem. It may thus suggest periods p that are too small to be used in practice. Better bounds can be derived if we for example use the structure of the saturation nonlinearity and that the smoothed dynamics is chosen to be exponentially stable.

5.2 Heuristic Tuning Rules

A practical issue that can be taken into account when tuning the dither period is how much fluctuations on the output we get due to the dither signal. We derive a heuristic bound on these fluctuations.

Assume the transients have decayed and signals are small enough, so that we can consider the linear range of the smoothed nonlinearity. Then the transfer function

$$G_{\mathrm{cl}}(s) = \left(1 + \frac{G(s)}{A}\right)^{-1} \frac{G(s)}{A},$$

where $G(s) = -c(sI - L)^{-1}b$, approximately describe the mapping from the dither signal to the output $y = -cx$. Choose $\omega_0 > 0$ such that

$$|G_{\mathrm{cl}}(j\omega)| \leq \frac{\mu}{A}, \quad \forall \omega \geq \omega_0, \tag{5}$$

for some small $\mu > 0$. Then we can expect $|y(t)| \leq \mu$ for sufficiently large t, if the dither period is chosen such that $p_0 \leq 2\pi/\omega_0$. The following heuristic tuning rule follows:

Step 1' Choose an output bound $\mu > 0$. Choose A based on (4) in Theorem 4.2.

Step 2' Choose p_0 such that $p_0 \leq 2\pi/\omega_0$, where ω_0 satisfies (5).

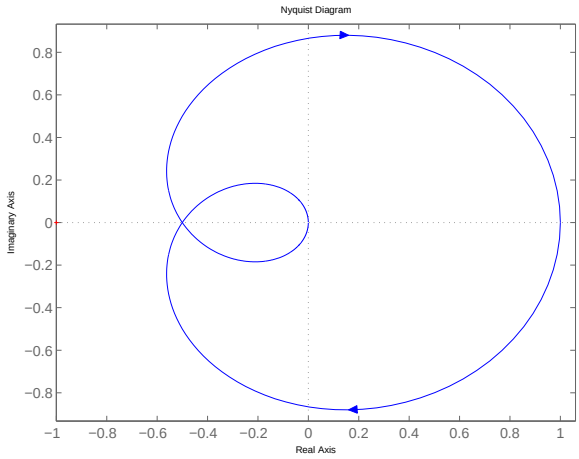

Figure 4: Nyquist curve of $G(s) = (1-s)(s+1)^{-2}$.

5.3 Example Revisited

Let us continue discussing the example in Section 3. Recall that

$$G(s) = -c(sI - L)^{-1}b = \frac{1-s}{(s+1)^2}.$$

Consider Theorem 4.2 with $H(s) = 0$, which corresponds to the circle criterion. We see from the Nyquist curve of G in Figure 4 that for $A > 0.56$

$$\operatorname{Re} G(j\omega) + A \geq 0, \ \forall \omega \in \mathbb{R}.$$

Hence, the dithered system is practically stable for $A > 0.56$ and p sufficiently small. By using Theorem 4.2 instead with $H(s) = -(s+1)^{-1}$, we can prove practical stability for $A > 0.501$. Figure 5 shows a simulation for $A = 0.502$ and $p = 1/10$. The system is close to the stability boundary. Recall that the smoothed system is unstable for $A < 0.5$.

Figure 6 shows the effect of the dither amplitude on the stability of the smoothed system: it is possible to obtain a fast convergence by increasing A. The upper plot shows a simulation for $A = 0.56$ and the lower $A = 0.70$.

Figure 7 shows finally the effect of the dither frequency on the approximation between the dithered system and the smoothed system: it is possible to obtain a response very close to the output of the smoothed system by decreasing the dither period. Compare the figure in Section 3.

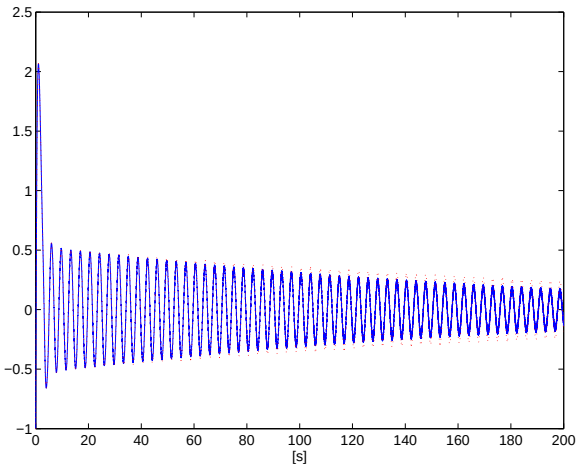

Figure 5: Outputs of the dithered (solid) and smoothed (dotted) systems close to the stability boundary predicted by Theorem 4.2. Note that in this figure the time axis extents to $t = 200s$.

6 Conclusions

In this paper we have shown how dither can be analyzed in nonsmooth systems. The main result is that a relay feedback system with a triangular dither signal at the input of the hard nonlinearity can be viewed as a feedback system (without dither) in which the relay is replaced by a saturation. While the amplitude of the dither signal affects the slope of the saturation, the approximate equivalence between the dithered and smoothed systems depends on the frequency of the dither signal. Explicit relations to achieve a desired approximation error have been given. Furthermore analytical and practical guidelines to design dithered systems have been presented. They were verified by simulations.

These preliminary results are the basis for future work that will include the analysis of relay feedback systems with the presence of other classes of dither signals. The analysis of the dither effect on other nonsmooth nonlinearities, such as quantizers, will also be studied in this context.

References

[1] G. Zames and N. A. Shneydor, "Dither in non-linear systems", *IEEE Transactions on Automatic Control*, vol. 21, no. 5, pp. 660–667, October 1976.

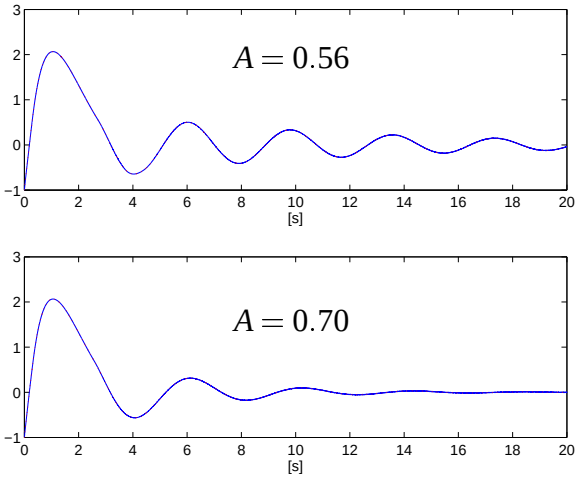

Figure 6: Output of the dithered system with δ having period $p = 1/50$. The amplitude is $A = 0.56$ (upper) and $A = 0.70$ (lower), respectively. A smaller A gives thus a less oscillating response.

[2] G. Zames and N.A. Shneydor, "Structural stabilization and quenching by dither in non-linear systems", *IEEE Transactions on Automatic Control*, vol. 22, no. 3, pp. 352–361, June 1977.

[3] S. Mossaheb, "Application of a method of averaging to the study of dither in non-linear systems", *International Journal of Control*, vol. 38, no. 3, pp. 557–576, September 1983.

[4] K.J. Åström and B. Wittenmark, *Adaptive Control*, Addison-Wesley, Reading, MA, 1989.

[5] B. Armstrong-Helouvry, *Control of Machines with Friction*, Kluwer Academic Publisher, Boston, 1991.

[6] B. Armstrong-Helouvry, P. Dupont, and C. Canudas de Wit, "A survey of models, analysis tools and compensation methods for control of machines with friction", *Automatica*, vol. 30, no. 7, pp. 1083–1138, 1994.

[7] A. V. Peterchev and S. R. Sanders, "Quantization resolution and limit cycling in digitally controlled pwm converters", in *Proc. IEEE Power Electronics Specialists Conf.*, Vancouver, Canada, June 2001.

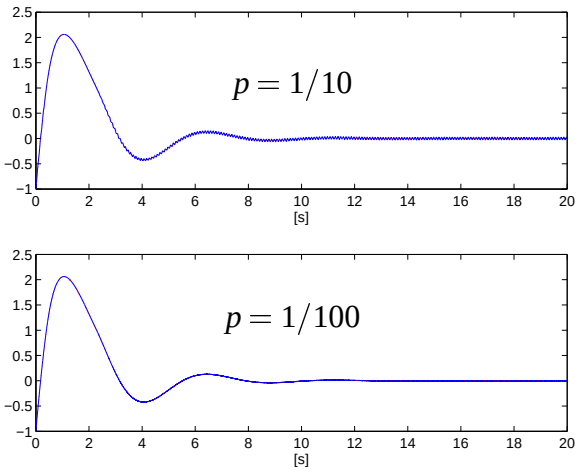

Figure 7: Output of the dithered system with δ having amplitude $A = 1$. The period is $p = 1/10$ (upper) and $p = 1/100$ (lower), respectively. A smaller p gives a better agreement between the responses of the dithered and smoothed systems.

[8] R.M. Gray and D.L. Neuhoff, "Quantization", *IEEE Transactions on Information Theory*, vol. 44, no. 6, pp. 2325–2383, 1998.

[9] Ya. Z. Tsypkin, *Relay Control Systems*, Cambridge University Press, Cambridge, UK, 1984.

[10] V.I. Utkin, *Sliding Modes in Control and Optimization*, Springer Verlag, Berlin, 1992.

[11] A. A. Pervozvanski and C. Canudas de Wit, "Asymptotic analysis of the dither effect in systems with friction", *Automatica*, vol. 38, no. 1, pp. 105–113, January 2002.

[12] D. Atherton, *Nonlinear Control Engineering*, Van Nostrand Reinhold Co., London, 1975.

[13] G. Zames and P.L. Falb, "Stability conditions for systems with monotone and slope-restricted nonlinearities", *SIAM Journal of Control*, vol. 6, no. 1, pp. 89–108, 1968.

[14] S. Sastry, *Nonlinear Systems: Analysis, Stability and Control*, Springer-Verlag, New York, 1999.

[15] A. Megretski and A. Rantzer, "System analysis via integral quadratic constraints", *IEEE Transactions on Automatic Control*, vol. 42, no. 6, pp. 819–830, June 1997.

[16] M. Vidyasagar, *Nonlinear Systems Analysis*, Prentice Hall, Englewood Cliffs, New Jersey, second edition, 1993.

A Proof of Theorem 4.1

Consider the dithered system (1) and the smoothed system (2) on the time interval $[0,T]$ and with $w(0) = x(0) = x_0$:

$$\dot{x}(t) = Lx(t) + bn(cx(t) + \delta(t)), \qquad x(0) = x_0 \tag{6a}$$

$$\dot{w}(t) = Lw(t) + bN(cw(t)), \qquad w(0) = x_0. \tag{6b}$$

Note that the right-hand side of (6a) is bounded on every compact time interval $[0,T]$, so there exists a positive constant M such that $|c\dot{x}(t)| \leq M$, for all $t \in [0,T]$. (An explicit estimate of M is given in the end of the proof.)

By integrating the two members of (6), we obtain

$$\begin{aligned} x(t) - w(t) = &\int_0^t [Lx(s) + bn(cx(s) + \delta(s))]ds \\ &- \int_0^t [Lw(s) + bN(cw(s))]ds \\ =&L\int_0^t [x(s) - w(s)]ds \\ &+ b\int_0^t [n(cx(s) + \delta(s)) - N(cw(s))]ds. \end{aligned} \tag{7}$$

The idea now is to show that the integral $\int_0^t [n(cx(s) + \delta(s))]ds$ can be approximated by $\int_0^t N(cx(s))ds$. The error introduced by this approximation is a function of the dither period p. We will show that it can be made small by decreasing the period p. This is not obvious, particularly, since n is a discontinuous nonlinearity.

We first evaluate the term $\int_0^t [n(cx(s) + \delta(s))]ds$. If we introduce $m = \lfloor T/p \rfloor$, the largest integer such that $mp \leq T$, then

$$\begin{aligned} \int_0^t n(cx(s) + \delta(s))ds = &\sum_{k=0}^{m-1} \int_{kp}^{(k+1)p} n(cx(s) + \delta(s))ds \\ &+ \int_{mp}^{mp+\Delta t} n(cx(s) + \delta(s))ds, \end{aligned} \tag{8}$$

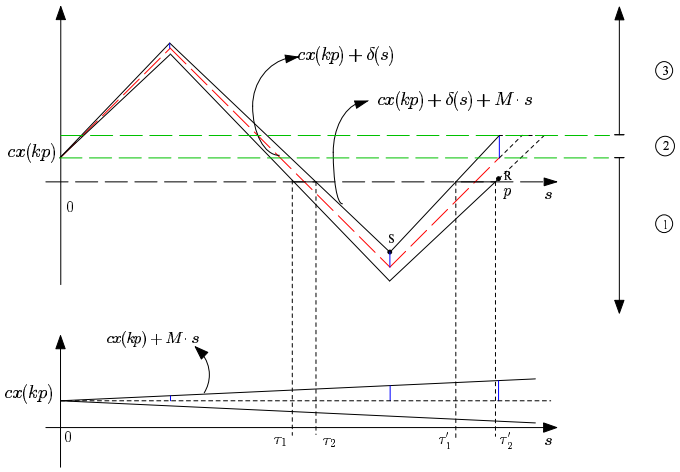

Figure 8: Time diagrams of the signals.

with $\Delta t = T - mp$. Since n is a bounded function and the time interval of the last integral in (8) has a Lebesgue measure less than p, we can write

$$\int_0^t n(cx(s)+\delta(s))ds = \sum_{k=0}^{m-1} \int_{kp}^{(k+1)p} n(cx(s)+\delta(s))ds + O(p). \tag{9}$$

Each term in the sum can be written as

$$\begin{aligned}
&\int_{kp}^{(k+1)p} n(cx(s)+\delta(s))ds \\
&\quad = \int_{kp}^{(k+1)p} n(cx(kp)+\delta(s))ds \\
&\qquad + \int_{kp}^{(k+1)p} [n(cx(s)+\delta(s)) - n(cx(kp)+\delta(s))]ds \\
&\quad = pN(cx(kp)) \\
&\qquad + \int_0^p [n(cx(s+kp)+\delta(s)) - n(cx(kp)+\delta(s))]ds.
\end{aligned} \tag{10}$$

Figure 8 illustrates the evolution for one dither period interval. In the top diagram, the solid lines bound $cx(s+kp)+\delta(s)$, $0 \le s \le p$. The dashed line is $cx(kp)+\delta(s)$. The figure presents all possible cases for the evolution of $cx+\delta$, in the sense that the envelope has the same characteristics as long as the point **R** is above the

point **S**. It is not difficult to show that this is equivalent to that the relation

$$p < \frac{1}{7} \cdot \frac{4A}{M} =: \bar{p} \tag{11}$$

holds. In the following we assume that p is chosen such that (11) holds.

All possible cases correspond to different values of $cx(kp)$ or, equivalently, all possible cases can be obtained by shifting the horizontal s-axis upward and downward in the top diagram of Figure 8. We have three cases:

$$\begin{cases} 0 \leq cx(kp) & \text{Region 1,} \\ cx(kp) \leq 0 \leq cx(kp) + Mp & \text{Region 2,} \\ cx(kp) + Mp \leq 0 & \text{Region 3.} \end{cases}$$

The regions are illustrated to the right in Figure 8 by the location of the s-axis for the three cases. The partition identifies the time intervals, during which the signal $cx(s+kp)+\delta(s)$ can have a zero-crossing. It is only during these intervals the integrand function in (10) can be non-zero. Introduce I_i to denote the sum of the lengths of these intervals for Region i, as further described below. Next we discuss each region separately.

Region 1: For the first region, I_1 can be the sum of at most two time intervals: $[\tau_1, \tau_2]$ and $[\tau_1', \tau_2']$, say. Since the considered signals are piecewise linear, the time instants τ_1 and τ_2 can be derived as

$$\tau_1 = \left(\frac{1}{2} + \frac{cx(kp)}{4A}\right) \frac{p}{1 + Mp/(4A)} \tag{12a}$$

$$\tau_2 = \left(\frac{1}{2} + \frac{cx(kp)}{4A}\right) \frac{p}{1 - Mp/(4A)}, \tag{12b}$$

and, analogously,

$$\tau_1' = \left(1 - \frac{cx(kp)}{4A}\right) \frac{p}{1 + Mp/(4A)} \tag{13a}$$

$$\tau_2' = \left(1 - \frac{cx(kp)}{4A}\right) \frac{p}{1 - Mp/(4A)}. \tag{13b}$$

Note that if the s-axis is below the point **S**, we have only one time interval. However, since we are only interested in an upper bound of I_1, we can consider the worst case, i.e., the case discussed previously. Moreover, if the s-axis is above the

point **R**, then τ_2' is less than p. However, we can still consider the previous expression, since the time interval $[\tau_1', \tau_2']$ derived above is greater than the effective one.

By considering the Lebesgue measures of the time intervals, we have

$$\tau_2 - \tau_1 = \left(\frac{1}{2} + \frac{cx(kp)}{4A}\right) \frac{M}{2A} \cdot \frac{p^2}{1 - (Mp/(4A))^2}, \tag{14}$$

and

$$\tau_2' - \tau_1' = \left(1 - \frac{cx(kp)}{4A}\right) \frac{M}{2A} \cdot \frac{p^2}{1 - (Mp/(4A))^2}. \tag{15}$$

Note two facts now: (i) the inequality (11) assures that $Mp/(4A)$ is always less than one, and (ii) if $Mp/(4A) \ll 1$ (i.e., $p \ll 4A/M$) the region in which the signal $cx(s+kp) + \delta(s)$ can lie is very small, so we can approximate the signal by $cx(kp) + \delta(s)$.

Hence, we have shown that the worst case (largest estimate of I_1) is when the integrand function in (10) is different from zero in both intervals $[\tau_1, \tau_2]$ and $[\tau_1', \tau_2']$. In that case we have

$$I_1 = \tau_2 - \tau_1 + \tau_2' - \tau_1' = \frac{3}{2} \cdot \frac{M}{2A} \cdot \frac{p^2}{1 - (Mp/(4A))^2}. \tag{16}$$

Region 3: Now we can consider the case in which the s-axis lies in the third region. The time interval $[\tau_1, \tau_2]$ is the same as previously in this case. The other possible time interval $[\tau_1'', \tau_2'']$ can be identified by considering the crossing of the first increasing part of the envelope through the s-axis. In an analogous way we can calculate the Lebesgue measure of the interval as

$$\tau_2'' - \tau_1'' = -\frac{cx(kp)}{4A} \cdot \frac{M}{2A} \cdot \frac{p^2}{1 - (Mp/(4A))^2}. \tag{17}$$

The worst case (through similar arguments as above) is given by

$$I_3 = \tau_2'' - \tau_1'' + \tau_2 - \tau_1 = \frac{1}{2} \cdot \frac{M}{2A} \cdot \frac{p^2}{1 - (Mp/(4A))^2}. \tag{18}$$

Note that both I_1 and I_3 are independent from the value of $cx(kp)$. The Lebesgue measure of the worst-case time interval is the same for all points in the corresponding region.

Region 2: Finally, we consider the second region. Here we can have a subtle behavior because it might happen that we have to consider three different time intervals. One of these, however, corresponds to the time interval considered in both Regions 1 and 3. Since we are carrying on a worst case analysis, it is possible to overcome the "loss of symmetry" by the following bound:

$$I_2 \leq I_1 + I_3 = 2 \cdot \frac{M}{2A} \cdot \frac{p^2}{1 - (Mp/(4A))^2}. \tag{19}$$

To conclude the discussion on Regions 1–3, note that the worst case I, say, for all three of them is bounded by the right-hand side of (19). It is easy to see that there exists $p^* > 0$ such that for all $p \leq p^*$, we have I of ordo p^2, i.e., $I = O(p^2)$. In particular, we may choose

$$p^* = \frac{4A}{M} \cdot \frac{\sqrt{2}}{2}, \tag{20}$$

so that

$$I \leq 4 \cdot \frac{M}{2A} p^2, \quad \forall p \leq p^*. \tag{21}$$

Note that (21) follows from (11). In conclusion, the estimate of the upper bound (21) is valid for all cases, so hence we have that (10) is equal to

$$\int_{kp}^{(k+1)p} n(cx(s) + \delta(s))ds = pN(cx(kp)) + O(p^2), \qquad p \leq \bar{p}.$$

So far we have mainly considered one period p. Since in (9) we have $m = \lfloor T/p \rfloor$ terms, we have

$$\int_0^t n(cx(s) + \delta(s))ds = \sum_{k=0}^{m-1} pN(cx(kp)) + O(p). \tag{22}$$

For p sufficiently small (or, equivalently, for m sufficiently large) the sum can be approximated by an integral. The maximum error of the approximation is related to the maximum slope of the signal $N(cx(s))$. But N satisfies the slope condition

$$0 \leq |N(cx(s_1)) - N(cx(s_2))| \leq \frac{M}{A} |s_1 - s_2|, \qquad \forall\, s_1, s_2 \in [0, T], \tag{23}$$

which implies

$$\int_{kp}^{(k+1)p} N(cx(s))ds = pN(cx(kp)) + O(p^2) \tag{24}$$

and, thus,

$$\sum_{k=0}^{m-1} pN(cx(kp)) = \int_0^{mp} N(cx(s))ds + O(p). \tag{25}$$

We have up to now proved that (7) can be written as

$$\begin{aligned} x(t) - w(t) =& L\int_0^t [x(s) - w(s)]ds \\ &+ b\int_0^t [N(cx(s)) - N(cw(s))]ds + O(p), \end{aligned} \tag{26}$$

for all $p \leq \bar{p}$. Since N has Lipschitz constant equal to $1/A$, we get

$$\begin{aligned} |x(t) - w(t)| \leq& \left(||L|| + \frac{|b| \cdot |c|}{A} \right) \\ &\times \int_0^t |x(s) - w(s)|ds + O(p). \end{aligned} \tag{27}$$

It is not difficult to show that if $p \leq \bar{p}$, an upper bound of the approximation error in (27) is actually

$$\left(\frac{9}{2} \cdot \frac{M}{A} T + 1 \right) |b| p. \tag{28}$$

Now, by applying the Grönvall-Bellman Lemma [14] to (27), we get for all $p \leq \bar{p}$,

$$\begin{aligned} |x(t) - w(t)| \leq& O(p) \\ &+ \int_0^t \left[\left(||L|| + \frac{|b| \cdot |c|}{A} \right) \right. \\ &\left. \times O(p) e^{\int_\tau^t \left(||L|| + \frac{|b| \cdot |c|}{A} \right) d\sigma} \right] d\tau \\ =& O(p) + \left(||L|| + \frac{|b| \cdot |c|}{A} \right) O(p) \\ &\times \int_0^t e^{\left(||L|| + \frac{|b| \cdot |c|}{A} \right)(t-\tau)} d\tau \\ =& O(p) + O(p) \left[e^{\left(||L|| + \frac{|b| \cdot |c|}{A} \right) t} - 1 \right]. \end{aligned} \tag{29}$$

Hence,

$$\begin{aligned}|x(t)-w(t)| \leq & O(p)e^{(\|L\|+|b|\cdot|c|/A)t} \\ \leq & O(p)e^{(\|L\|+|b|\cdot|c|/A)T} = \varepsilon, \quad \forall t \in [0,T]. \end{aligned} \tag{30}$$

This concludes the proof of the theorem.

Note that from (28), we have an estimate of p_0 of the theorem, namely,

$$p_0 = \min\left(\frac{4A}{7M}, \frac{\varepsilon}{(9MT/(2A)+1)\,|b|e^{(\|L\|+|b|\cdot|c|/A)T}}\right) \tag{31}$$

We finally present an explicit estimate for M: Note that the smoothed system (2) has a bounded solution $w(t)$ on a finite time interval $[0,T]$, so there exists $d>0$ such that $|w(t)| \leq d$, for all $t \in [0,T]$. A possible choice of M (the bound of $|c\dot{x}|$) based on (1) and (31) is

$$M = \|L\|(d+\varepsilon) + \frac{|b|\cdot|c|}{A}. \tag{32}$$

B Proof of Theorem 4.2

The saturation nonlinearity $N(z)$ satisfies the integral quadratic constraint

$$\int_0^\infty [z(t) - AN(z(t))][N(z(t)) - (h * N(z))(t)]\,dt \geq 0, \qquad \forall z \in \mathbf{L}_2[0,\infty),$$

where $*$ indicates the convolution product. If the criterion (4) holds, then it follows from the main result in [13, 15] that the smoothed system in (2) is $\mathbf{L}_2$-stable. Moreover, since the vector field of (2) is Lipschitz continuous it can be shown that $\mathbf{L}_2$-stability implies exponential stability [15, 16]. Hence, there exists $\alpha_0 > 0$ and $\beta_0 \geq 1$ such that

$$|w(t)| \leq \beta_0 e^{-\alpha_0 t}|x_0|, \quad \forall t \geq 0.$$

We will use this to prove practical stability of (1). We iteratively consider time intervals of length T and, in order to guarantee a decay rate of 0.1, we choose $T = -{\alpha_0}^{-1}\ln(0.1/\beta_0)$. Then, if p_0 is sufficiently small (see (31)), we have

$$|x(t)-w(t)| \leq \varepsilon_0$$

on $t \in [0,T]$. If we consider a new smoothed system satisfying (2) on the time interval $[kT,(k+1)T]$, $k = 0,1,2,\ldots$, with initial condition $w(kT) = x(kT)$, then it follows from the above arguments that

$$|w(t)| \leq \beta_0 e^{-\alpha_0(t-kT)}|x(kT)|, \quad \forall t \geq kT,$$

and, by applying Theorem 4.1 again,

$$\begin{aligned} |x(t)| =& |x(t) - w(t) + w(t)| \leq \varepsilon_0 + |w(t)| \\ \leq& \beta_0 e^{-\alpha_0(t-kT)}|x(kT)| + \varepsilon_0 \end{aligned} \tag{33}$$

on $t \in [kT,(k+1)T]$. By evaluating (33) in $t = (k+1)T$,

$$|x[(k+1)T]| \leq 0.1|x(kT)| + \varepsilon_0. \tag{34}$$

Hence

$$|x(kT)| \leq 0.1^k |x_0| + \varepsilon_0 \frac{1-0.1^k}{1-0.1}. \tag{35}$$

Then (33) becomes

$$\begin{aligned} |x(t)| &\leq \beta_0 e^{-\alpha_0(t-kT)} \left(e^{-\alpha kT}|x_0| + \frac{\varepsilon_0}{0.9} \right) + \varepsilon_0 \\ &\leq \beta_0 e^{-\alpha_0(t-kT)} e^{-\alpha kT} |x_0| + \underbrace{\beta_0 \frac{\varepsilon_0}{0.9} + \varepsilon_0}_{\varepsilon}, \end{aligned} \tag{36}$$

where $\alpha = -T^{-1}\ln 0.1$. Since $\alpha_0 > \alpha$ and $t \geq kT$, (36) becomes

$$|x(t)| \leq \beta_0 e^{-\alpha t} |x_0| + \varepsilon. \tag{37}$$

We have thus shown practical stability with $\alpha = -T^{-1}\ln 0.1$ and $\beta = \beta_0$.